A PARALLEL PLATE AVALANCHE CHAMBER WITH A RESISTIVE GERMANIUM ANODE AND A TWO DIMENSIONAL READ-OUT

R.Bellazzini, C.Betti, A.Brez, E.Carboni, M.M.Massai and M.R.Torquati
Dipartimento di Fisica dell'Università di Pisa and INFN - Sezione di Pisa
Via Livornese, 582/A - San Piero a Grado - 56010 - PISA (Italy)

Abstract

A novel type of parallel plate counter with a resistive anode and a two dimensional read-out is presented. The anode is made of a thin germanium layer with a sheet resistivity $\gtrsim$ 1 M$\Omega/\square$ and the cathode is made of aluminized mylar 5 μm thick. The anode is transparent to the fast impulse due to the collection of the multiplication electrons. A chessboard of "pads" placed behind the anode plane is used to obtain the positional information. The detector and the read-out system are physically and logically separated. The device is continuous, homogenous, self-triggering and can operate at a rate of 10^6 particles/s. A spatial resolution $\lesssim$ 50 μm for both coordinates has been measured.

Introduction

In many low or high energy physics experiments it is often necessary or desirable to measure with a high resolution the three spatial coordinates of the impact point of an ionizing particle with a single detector. Normally this cannot be achieved with wire chambers because the resolution in the direction orthogonal to the wires is severely limited by the wire pitch. A solution to this problem could be found by using a continuous and homogeneous detector, like a parallel plate counter, but still preserving the positional sensitivity typical of discrete structures.

Parallel plate counters have been used for several years in nuclear physics as detectors of highly ionizing particles (1, 2, 3, 4). Their main features are : 1) very good time resolution, 2) high data - rate capability, 3) total insensitivity to radiation damage. Their major drawback is the null or poor position sensitivity and the low detection efficiency for minimum ionizing particles when operated at low gas pressure. To overcome these problems we have designed, built and tested a new type of parallel plate avalanche chamber. This detector has a resistive anode and a high resolution two-dimensional read-out and works at atmospheric or higher pressure. Because of its high resistivity the anode is transparent to the fast impulse generated by the avalanche electrons. Behind the anode plane a chessboard of "pads" collects this fast impulse and it is used to obtain the position sensitivity.

Our detector essentially behaves like a wire chamber without wires. In this respect it differs significantly from other detectors based on the same principle such as those proposed by Y.N.Pestov and G.V.Fedotovich (5) and by R.Santonico and R.Cardarelli (6). The main differences are that our detector operates : a) at much lower values of the reduced electric field, b) at a gas gain lower by factor $> 10^3$ and at lower electrode resistivity. All these factors combine to give a much higher rate capability to the device we have developed.

In this paper the principle of operation and the results of laboratory tests of this detector are presented.

Principle of operation of the detector

Gas gain

A parallel plate chamber (PPC) consists of two continuous electrodes mounted parallel to each other (see fig. 1). When a potential difference is applied between close electrodes, a uniform, intense, electric field is established inside the detector volume. Ionization electrons delivered by a traversing particle start to multiply until they are collected by the anode. In the case of a point ionization the number of secondary electrons is given by :

$$n = n_o e^{\alpha d} \qquad (1)$$

with

n_o=number of primary electrons

d=drift lenght

α =first Townsend coefficient.

Ionization collisions close to the cathode give a greater contribution to the total signal than those close to the anode. A gas gain up to 10^4 - 10^5 can be easily obtained. The signal as an amplitude of a few hundredths of microVolts and consists of two parts :

1) a fast rising component due to the collection of the electrons :
2) a slowly rising component due to the positive ions with their much lower drift velocity.

The resistive anode

If the electrode plates are both made of a conducting material a voltage pulse due to the collection of the drifting charges can be observed in a external circuit connected to one of the electrodes. However, bacause the whole electrode plane moves to the new potential no positional information can be obtained from this signal.

The situation is completely different if one or both of the electrodes are made of a semiconductor material with a sufficiently high sheet resistivity. In this case we can consider the electrode as a two dimensional array of resistances (7). If an array (one or two-dimensional) of capacitances is placed behind the resistive plane a "short-circuit" to ground is established for impulsive current (see fig. 2). We can say that the resistive plane acts as a conductor for d.c. currents, so that it can be charged to a suitable potential, while it acts as a dielectric for very short currents so that it is transparent to

0018-9499/86/0200-0267$01.00©1986 IEEE

the corresponding impulses. The positional information can be obtained from the distribution of the charge collected on the external capacitances.

Detector design and construction

The material we choose for the construction of the resistive electrode is germanium. Germanium has a bulk resistivity of 60 Ω.cm so that a 0.1-0.01 μm thick deposit obtained via vacuum evaporation results in a sheet resistivity in the range in 6-60 MΩ /$\square$ which is high enough to ensure the full transparency to the signals coming from the detector. Further advantages of the vacuum avaporation are the high uniformity of the deposit ($\pm$1%) and the easily controllable value of the resistivity which is a function only of the thickness of the deposit. The high uniformity of the sheet resistivity allows one to work at values of resistivity close to the one corresponding to the full transparency threshold, thus reducing the rate limitations of the device.

As a support of the germanium deposit we used machined epoxy planes or polished glass. The cathode is made of aluminized mylar 5 μm thick. This light material was chosen to have an entrance window for short range particles such as low energy X or β^- rays. The gap between the anode and the cathode was obtained with spacers made of epoxy having a thickness in the range of 1-3 mm. Special care was taken to ensure good uniformity of the electrode plates and of the interelectrode gap ($\pm$0.005 mm tolerance). Behind the anode plane a double-sided chess board of 2 mm x 2 mm "pads" collects the fast electron impulse and is used to obtain the event position. Half of the pads are zig-zag connected to form rows on one side of the chess-board. Metallized holes of 0.5 mm diameter connect the remaining half of the pads to form columns on the back side of the chess board. In this way a two dimensional read-out is obtained looking at the detector from one side only, leaving the front side free as a window for the incoming particles.

The detector active area is 13 cm x 13 cm and the gas filling was Argon (90%)-Methane (10%). A typical operating voltage when working at normal pressure and with a ^{55}Fe illumination was 3.2 KV corresponding to a uniform electric field of 16.0 KV/cm for a 2 mm gap.

The advantages of this set-up are :

1) two dimensional positional information is obtained from a perfectly homogenous, self triggering detector ;
2) the detector and the read-out system are physically and logically separated so that they can be optimized independently ;
3) the data-rate is subdivided over the whole detector volume ;
4) because the cathode is the entrance window and the electrons created close to the cathode have the largest gain, an "electronic collimation" of inclined tracks is obtained ;
5) the detector is mechanically very simple and sturdy (no fragile wires etc...).

The read-out system

The event position is obtained from the measurement of the centroid of the charge distribution on the read-out pads. The electronic chain consists of a low noise charge pre-amplifier (8), a linear amplifier with a 2 μs Gaussian shaping and a peak-sensing ADC for each row and column. The data acquisition is started and gated by the prompt signal obtained from the cathode plane. The distance of the read-out plane from the anode plane can be easily adjusted depending on the pitch of the rows and columns. The relative gains of each channel were equalized within 1%. To find the value of the event position we have adopted two different algorithms. The first is the direct calculation of the center of gravity of the measured distribution obtained trough the relation $\bar{X} = \Sigma_i Q_i X_i / \Sigma_i Q_i$ while the second relies on the shape of the charge distribution (9). If Q_j is the channel containing the maximum of the charge distribution, we can define $R^+ = Q_{j+1}/Q_j$ and $R^- = Q_{j-1}/Q_j$. Both R^+ and R^- are functions of x_j the true event position inside the strip i, that is $R^+ \equiv R^+(x)$ and $R^- \equiv R^-(x)$. If the theoretical dependence upon x of $R^+(x)$ and $R^-(x)$ is known from a model of the induction process, then the measured values R^+ and R^- allow a determination of the event position. The electrostatic distribution of the charge induced by a point charge placed between the cathode and the read-out plane was shown to reproduce the measured distribution and was used to obtain the value of the estimator of the true event position (10, 11). Fig. 3 shows the scatter plot of R^- versus R^+ as measured in our chamber with superimposed the theoretical fit obtained from the electrostatic model of the charge induction. The best estimate of the avalanche position is given by the intersection of the theoretical curve with the line connecting the data point and the point (1,1). The two reconstruction algorithms give roughly the same results. The algorithm exploiting the shape of the charge distribution has the additional advantage that, unlike in the center of gravity method, the differential non linearity does not depend so strongly on the ratio of the strip pitch to the distance between the anode and the read-out plane. For a more detailed discussion of the reconstruction algorithms and their relative merits we refer to a forthcoming paper (12).

Results

The results described in this paper refer to the operation of the chamber at standard pressure. The chamber has also been operated for some time at 2 atm. absolute pressure without any particular problem.

Fig. 4 shows the typical current signal on the cathode plane when a detector with a 2 mm gap is irradiated with a ^{55}Fe source. The fast electron component and the slow tail due to the collection of the positive ions are apparent. The electronic amplification was A=500. The height of the plateau in fig. 4 is proportional to the ion current component $i = n_o \exp(\alpha d)/T$ where T is the duration of the ion collection process (5 μs in this case). Because the preamplifier has an input impedance Z=500Ω ,we can use the result of fig. 6 to estimate the gas gain

$G=\exp(\alpha d)=VT/AZn_o e$ where V is the maximum output voltage, n_o the number of primary electrons created at the cathode (=200 for ^{55}Fe) and e is the electron charge. A gas gain factor $G \approx 10^5$ can be estimated for d=2 mm. Fig. 5 shows the fast component of the signal after differentiation of the slow component. The differentiation time constant was τ = 500 ns.

Fig. 6 shows the pulse height spectrum of the signal of fig. 4. The spectrum is almost continuous because for each conversion point there is a different gain according to the law $G \propto \exp(\alpha d)$. Fig. 7 shows the dependence of the counting rate (singles) on the operating voltage for a collimated ^{90}Sr source emitting β^- rays with an end point energy of 2.27 MeV. The PPC had a 2 mm gap. To have just an idea of the detection efficiency we have exposed a plastic scintillator to the same ^{90}Sr source. The global counting rate measured with the PPC was comparable with the one obtained using the scintillator.

The uniformity of response was checked moving a ^{55}Fe point source across the detector. Fig. 8 shows the measured counting rate as a function of the source position.

To measure the spatial resolution in one coordinate we have built a resolution phantom constituted of two slits 230 μm wide, 1 mm apart, which were uniformely illuminated with a ^{55}Fe source. Fig. 9 shows the histogram of the centroid distribution as measured with the center of gravity method. The width (FWHM) of the peaks is $\sim$ 250μm indicating that the resolution is much better than the slit width. To have a quantitative estimate of the resolution we have used a mathematical model. We have assumed that the histogram of fig. 9 is the result of the convolution product of a square wave with a gaussian function. The resolution is the width of that gaussian function which, when convoluted with the square wave gives the best fit to the data of fig. 10. The resulting spatial resolution is compatible with a σ = 50 μm.
This figure does not represent the intrinsic resolution of the device but the contribution to the resolution of the finite range of the primary photoelectrons created by the interaction of the 5.9 Kev ^{55}Fe X-rays with Argon.

The integral and the differential non linearity were studied by moving the two slits across the central (instrumented) part of the detector by means of a micrometric screw. The maximum absolute position error and the maximum differential nonlinearity were found 75 μm and 4% respectively (see fig. 10a and fig. 10b). To study the two dimensional reconstruction capability of the device we have utilized a resolution phantom which is shown in fig. 11 together with the reconstructed image. In this later case the charge-ratio algorithm was utilized.

Rate limitations

Resistive plate chambers could suffer from rate problems (7). A voltage drop $V \propto I \cdot R \cdot N$ due to the discharge process occurs when N particles/s interact with the device, I being the equivalent d.c. current due to the detection of one particle per second and R the total mean resistance of the anode plate. In our case the situation is quite favourable because the detector is operated at very low gas gain (10^4 - 10^5) and $I \approx 10^{-12}$ A/p/s. If R is in the range 1-10 MΩ and a voltage drop of 1 V is tolerated, a data rate $N \sim 10^5$ - 10^6 p/s is allowed.

Conclusions

A new type of position sensitive detector has been presented. The device is continuous, homogeneous, self-triggering and can operate at a rate of 10^6 particles/s. A resolution of 50 μm for both coordinates has been measured. Further tests of efficiency, time resolution and uniformity of response to minimum ionizing particles are planned for the near future.

Acknowledgments

We thank G. Favati of INFN - Pisa for the accurate mechanical work and G. Muratori of CERN for his hospitality during the precise machining of the epoxy plates.

References

(1) G. Hempel et al., Nucl. Instr. and Meth., 131 (1975) 445.
(2) H. Stelzer, Nucl. Instr. and Meth., 133(1976) 409.
(3) D.V. Harrack and H.J. Specth, Nucl. Instr. and Meth., 164 (1979) 477.
(4) J. Hendrix, IEEE Trans. Nucl. Science, Vol. NS-31, N.1 (1984) 281.
(5) Yu.N.Pestov and G.V.Fedotovich,Preprint IYAF 77-78,SLAC Translation 1849(1978).
(6) R. Santonico and R. Cardarelli, Nucl. Instr. and Meth., 131 (1975) 445.
(7) G. Battistoni et al., Nucl. Instr. and Meth., 202 (1982) 459.
(8) V. Radeka, IEEE Trans. Nucl. Science, Vol. NS-21, N.1 (1974) 51.
(9) J. Chiba et al., Nucl. Instr. and Meth., 206 (1983) 451.
(10) W.R. Smyth, 'Static and Dynamic Electricity', MacGraw Hill, New York (1968).
(11) R. Bellazzini et al., Nucl. Instr. and Meth., 225 (1984) 145.
(12) R. Bellazzini et al., to be submitted to Nucl. Instr. Methods.

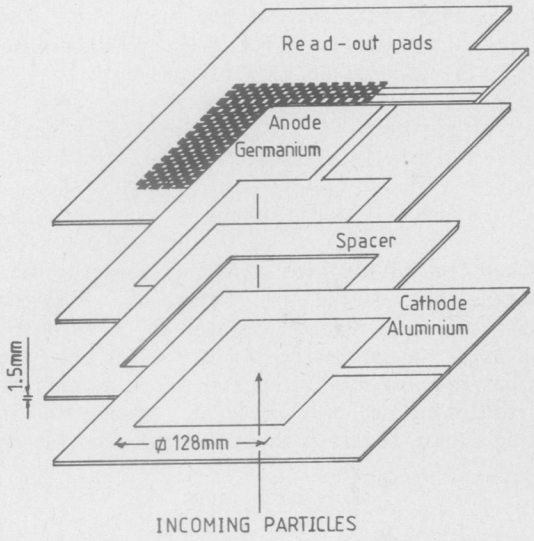

Fig. 1) : Prospective view of the detector assembly

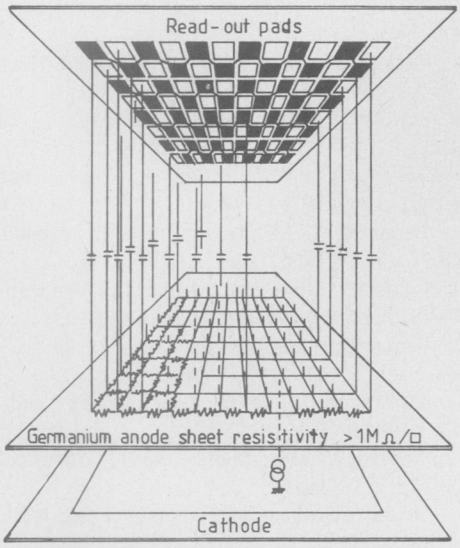

Fig. 2) : Electric a rapresentation of the anode transparency concept

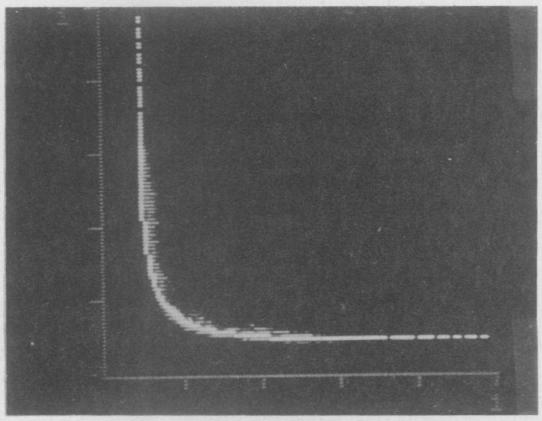

Fig. 3) : Scatter plot of Q_{i-1}/Q_i versus Q_{i+1}/Q_i with superimposed the theoretical fit obtained from the electrostatic model of charge induction

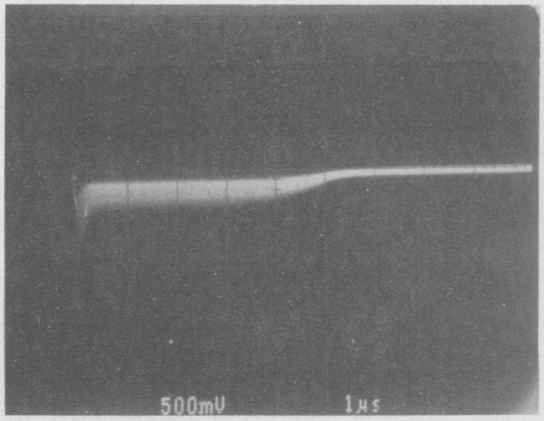

Fig. 4) : The typical current signal on the cathode plane when the detector is irradiated with a ^{55}Fe source

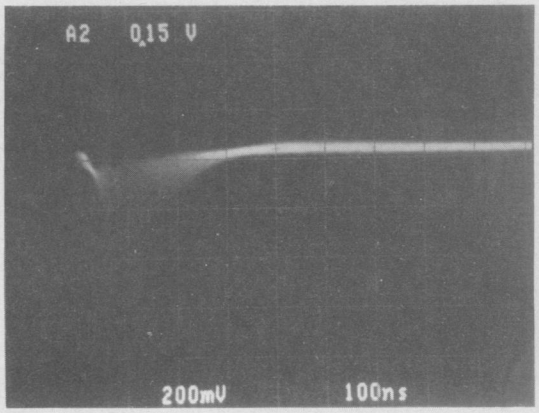

Fig. 5) : The electron component of the signal observed after differentiation of the signal of fig. 4

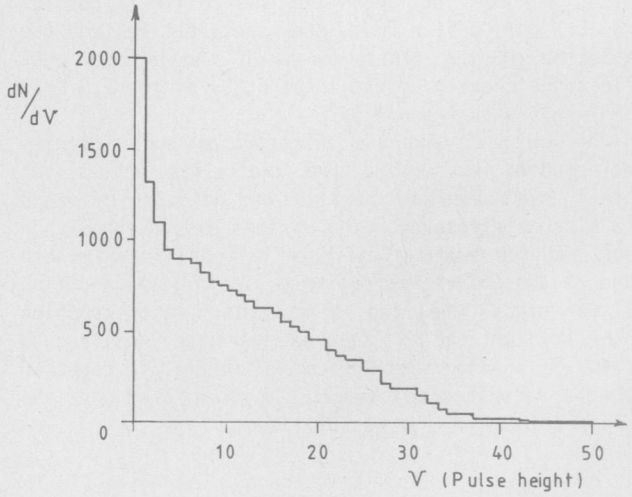

Fig. 6) : Pulse height spectrum of the signal of fig. 4

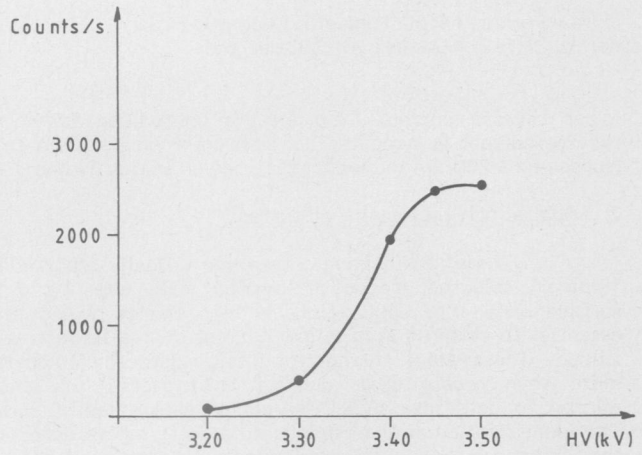

Fig. 7) : The dependence of the counting rate on the operating voltage when the chamber is irradiated with a ^{90}Sr source

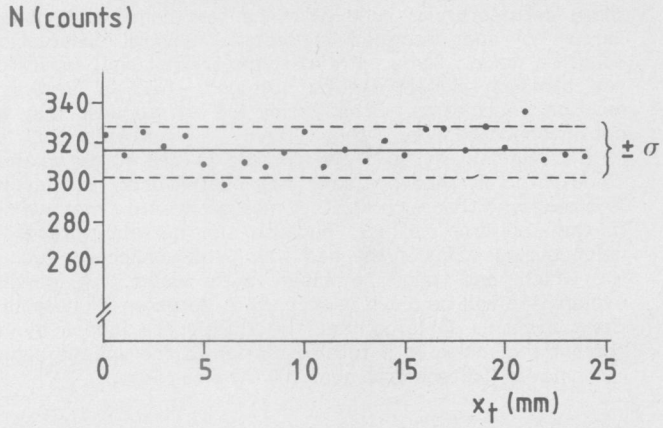

Fig. 8) : The uniformity of response of the detector

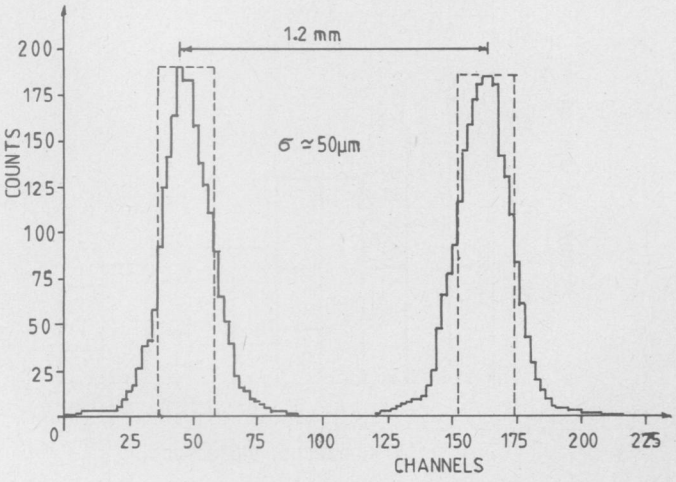

Fig. 9) : Histogram of the centroid distribution measured when two slits 230 μm wide and 1 mm apart were uniformely irradiated with a ^{55}Fe source. The dotted line represents the slit width

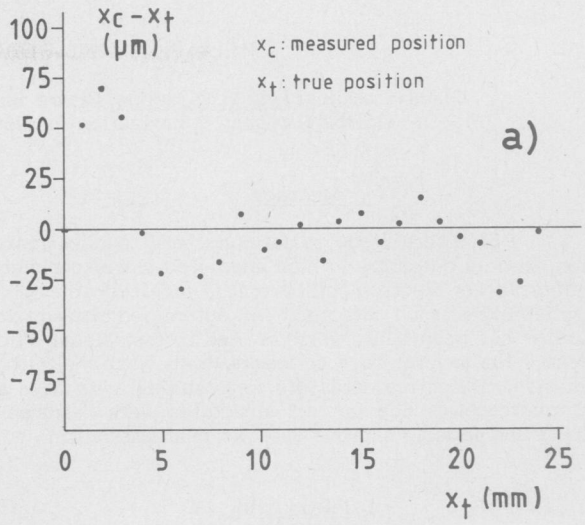

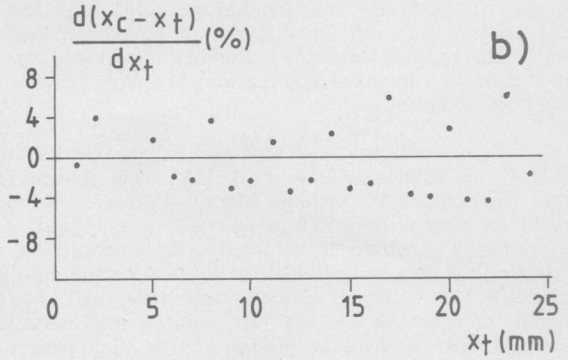

Fig. 10) a: The integral linearity
b: The differential linearity

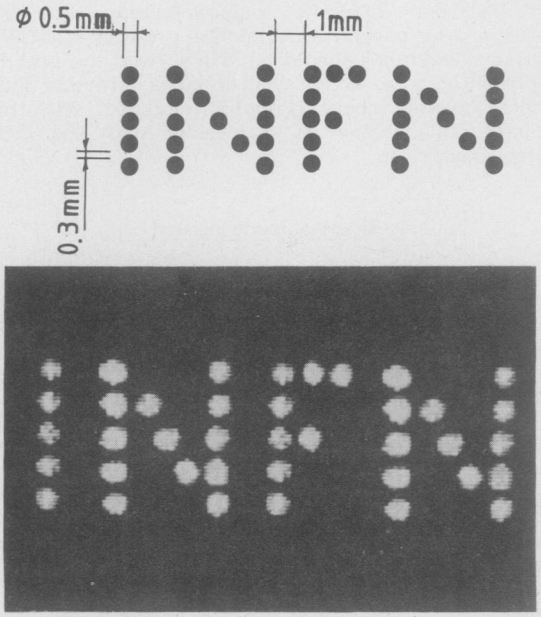

Fig. 11) upper: Resolution phantom constituted of 39 holes of 0.5 mm diameter, 0.3 mm apart arranged to form the word INFN
lower: The reconstructed image (^{55}Fe source)